Published by IOP Publishing for Sissa Medialab

Received: *October 30, 2020*
Accepted: *December 2, 2020*
Published: *January 27, 2021*

Measurement of the radiation environment of the ATLAS cavern in 2017–2018 with ATLAS-GaAsPix detectors

I. Boyko,[a] **P. Burian,**[e,f] **M. Campbell,**[b] **G. Chelkov,**[a,d,1] **E. Cherepanova,**[a] **B. Di Girolamo,**[b] **A. Gongadze,**[a] **J. Janecek,**[e] **D. Kharchenko,**[a] **U. Kruchonak,**[a] **A. Lapkin,**[a] **Y. Mora Sierra,**[e] **M. Nessi,**[b] **L. Pontecorvo,**[b] **S. Pospisil,**[e] **D. Rastorguev,**[a,d] **V. Rozhkov,**[a] **P. Smolyanskiy,**[a,e] **M. Suk,**[e] **I. Stekl,**[e] **O. Tolbanov,**[c] **A. Tyazhev**[c] **and A. Zarubin**[c]

[a] *Joint Institute for Nuclear Research, Dubna, Russia*
[b] *CERN, Geneva, Switzerland*
[c] *Tomsk State University, Tomsk, Russia*
[d] *Moscow Institute of Physics and Technology, Dolgoprudny, Russia*
[e] *Institute of Experimental and Applied Physics, Czech Technical University, Prague, Czech Republic*
[f] *Faculty of Electrical Engineering, University of West Bohemia, Pilsen, Czech Republic*

E-mail: chelkov@jinr.ru

Abstract: A network of ten GaAs:Cr semiconductor Timepix detectors with GaAs:Cr sensors was installed in the ATLAS cavern at CERN's LHC during the shutdown periods 2015–2016 and 2016–2017 in the framework of a cooperation between ATLAS and the Medipix2 Collaboration. The purpose was to augment the existing system of measuring and characterising the radiation environment in the ATLAS cavern that is based on ATLAS-TPX devices with pixelated silicon sensors. The detectors were in continuous operation during 13 TeV proton-proton collisions in 2017–2018. Data were recorded during proton-proton bunch crossings, and during times without bunch crossings (LHC physics runs) as well as between the physics runs. The overall level of particle radiation as well as the ratio between neutral and charged particles were measured. The detectors recorded all interactions of charge particles, neutrons and photons in GaAs sensors, in which the signal was higher than 6.5 keV in individual pixels. This made it possible to register clusters (tracks) of individual radiation particles interacting in the detectors sensors. During LHC beam-beam collisions, these were all particles represented in the radiation field. In the periods without beam-beam collisions, these were photons and electrons resulting from radioactivity induced during previous collisions in GaAs detectors and in surrounding construction materials, namely by neutrons.

Keywords: Radiation monitoring; Particle tracking detectors (Solid-state detectors); Solid state detectors; Pixelated detectors and associated VLSI electronics

[1]Corresponding author.

https://doi.org/10.1088/1748-0221/16/01/P01031

2021 JINST 16 P01031

Contents

1 Introduction

A network of ten hybrid pixel detectors consisting of GaAs:Cr [1] semiconductor sensor layers bump-bonded to Timepix readout chips [2], referred as the network of ATLAS-GaAsPix detectors [3], was installed in the ATLAS cavern of the LHC at CERN during the ATLAS shutdown periods 2015–2016 and 2016–2017. The project was carried out by the Joint Institute for Nuclear Research and the Institute of Experimental and Applied Physics of the Czech Technical University in Prague with the support by the ATLAS and the Medipix collaborations. The GaAs:Cr sensors for detectors were provided by Tomsk State University. The installation of the ATLAS-GaAsPix network was inspired by the results obtained from the network of ATLAS-MPX detectors installed in 2008–2011 [4, 5]. This network was intended to augment the existing system of 15 hybrid pixel detectors consisting of Si semiconductor sensor layers bump-bonded to Timepix readout chips, referred as the ATLAS-TPX system [6]. This system was installed in 2013 to measure and characterise the radiation environment in the ATLAS cavern [7, 8].

The salient feature of the present work is the supplement of the Si (atomic number $Z = 14$) of the ATLAS-TPX detector system by GaAs compensated with Cr. The use of GaAs is motivated by its substantially better detection efficiency for photons (the atomic numbers of Ga and As are $Z = 31$ and $Z = 33$, respectively) and its potential for measuring the neutron fluence, i.e. the time-integrated neutron flux density. The better photon and X-ray detection efficiency of GaAs with respect to Si is highlighted in figure 1 as well as its higher neutron capture cross-section. Higher X-ray registration efficiency determines the main GaAs:Cr detector field of application — X-ray imaging [9–12]. Also, the GaAs:Cr based Timepix detectors could benefit in charge particle tracking due to their higher stopping power [13].

2021 JINST 16 P01031

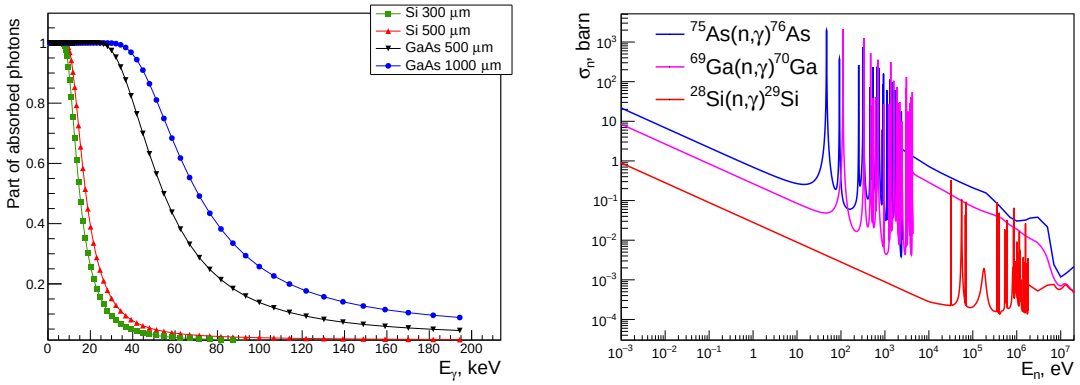

(a) (b)

Figure 1. (a) X-ray and gamma absorption efficiency of GaAs and Si sensors of various thicknesses. (b) The cross sections for neutron capture [14] of ^{28}Si, ^{69}Ga and ^{75}As.

2 The ATLAS-GaAsPix detector

The ATLAS-GaAsPix detector is a hybrid detector (see figure 2) consisting of a pixellated GaAs:Cr sensor layer bump-bonded to a Timepix readout chip. The Timepix chip [2] has been developed by the Medipix Collaboration as an evolution of the Medipix2 chip and has larger functionality. Each pixel can be programmed to either count hits, to record time-over-threshold, or to measure the arrival time of the first particle hitting a pixel. A common shutter signal determines when all pixels are active.

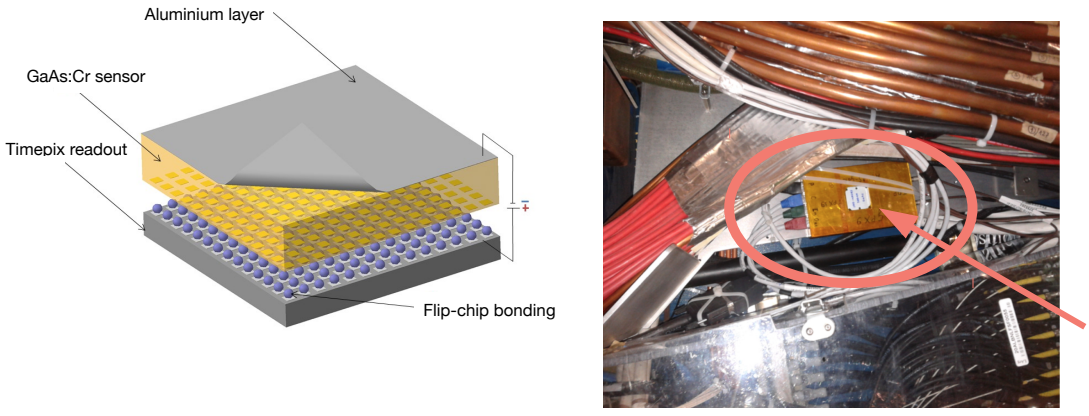

(a) (b)

Figure 2. (a) Schematic view of the hybrid GaAsPix detector. Aluminum layer serves as an electrode. (b) Photograph of a GaAsPix detector installed in the ATLAS cavern.

The ATLAS-GaAsPix detectors were operated in the time-over-threshold mode permitting the measurement of the energy deposited by a radiation quantum in a single pixel. If the deposited energy exceeds a preset energy threshold, one or several pixels are activated forming a cluster of adjacent pixels. The data were recorded as a set of images ("frames") which contain the status of

2021 JINST 16 P01031

all the $256 \times 256 = 65536$ pixels after a selected exposure time (typically 10 ms to 1 s) which was adjusted according to the local particle flux.

Five of the ATLAS-GaAsPix detectors (GPX1-GPX5) are single-layer detectors with a sensor thickness of 500 µm or 1000 µm (see table 1 and figure 3a). The remaining five detectors of the ATLAS-GaAsPix network (GPX6-GPX10) are twin detectors, which consist of two sensor layers (500 µm or 1000 µm thick) arranged as shown in figure 3b. The detectors are operated with an external bias voltage up to -500 V.

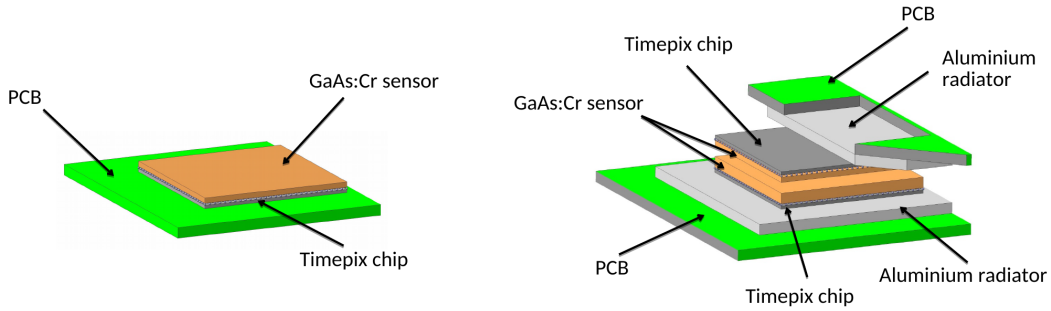

(a) (b)

Figure 3. Sketch of single (a) and twin (b) GaAsPix detector assemblies.

The readout hardware design of the network is a copy of the ATLAS-TPX system, which was developed and installed by the Institute of Experimental and Applied Physics of the Czech Technical University in Prague [5, 6]. The system is designed for remote operation with a distance between the detectors and the readout electronics of up to 100 m. The maximum frame rate of the system is 16 per second.

To prevent mechanical damage each ATLAS-GaAsPix detector is enclosed in an aluminum box (see figure 2b). The box for single layer detectors has an entrance window located on the sensor side of the detector. The box for a twin detector has an entrance window above and below the stack.

The coordinates of the ten GaAsPix detectors installed in the ATLAS cavern are given in table 1. The x, y and z axes correspond to the standard right-handed ATLAS coordinate system: z along the beam direction with the positive sign corresponding to side A, the opposite direction is corresponding to side C; the positive sign of y corresponds to the up direction, the positive sign of x points to the centre of the LHC ring; (0,0,0) are the coordinates of the nominal interaction point.

2.1 Detector response

Particles leave traces of different shapes in the detectors while they interact in the sensitive volume of the sensor. The groups of pixels located side by side composes a cluster or an event. The composition, size and shape of active clusters produced in the GaAsPix detectors by these particles depend on their parameters: the type of particles, their energies, incident angles, and the nature of their interactions in the detector. During the ATLAS-GaAsPix detectors operation a sequences of frames with registered events on it are recorded. An example of one frame taken at the time of beam collisions is shown in figure 4.

2021 JINST 16 P01031

Table 1. Sensor thicknesses and locations of the ATLAS-GaAsPix detectors in the ATLAS cavern. X, Y, Z axes correspond to the standard ATLAS coordinate system. The orientation of the devices is given as an angle between Z-axis and the detector sensor plane.

Detector ID	Sensor thickness (µm)	X (m)	Y (m)	Z (m)	Orientation
GPX1	500	-5.98	0	7.22	90°
GPX2	1000	-5.80	0	7.22	90°
GPX3	1000	-16.69	-0.06	5.07	0°
GPX4	500	0	-0.28	-6.74	0°
GPX5	500	0	1.57	-12.86	90°
GPX6	1000/500	-1.12	-0.21	3.53	0°
GPX7	1000/500	0.65	-1.45	7.8	0°
GPX8	1000/1000	0	1.57	15.09	90°
GPX9	1000/500	-3.46	-0.92	2.84	0°
GPX10	1000/500	-3.46	-0.92	-2.84	0°

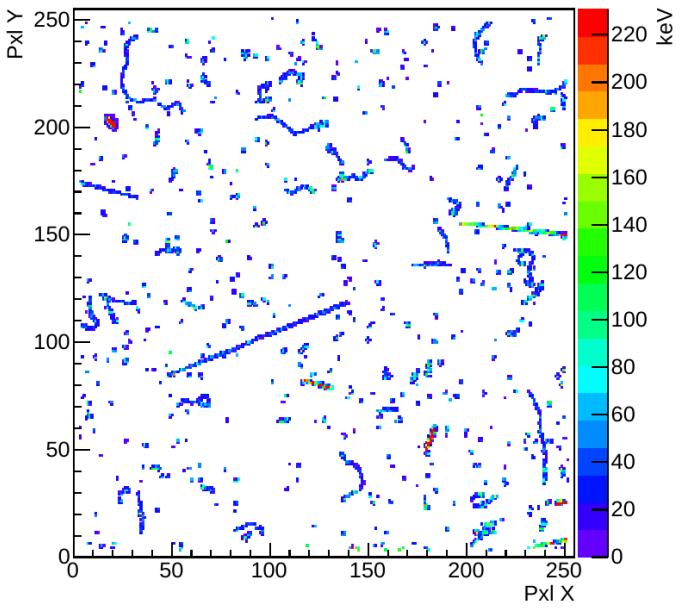

Figure 4. A typical frame recorded by the ATLAS-GaAsPix detector during LHC collisions.

The radiation environment in the cavern comprises primarily γ's, electrons, muons, pions, kaons, neutrons and protons [15]. Photons and X-rays are detected indirectly via one of the interactions: photoelectric effect, Compton scattering and pair creation. That causes the similar shapes of clusters for electrons and photons. A size and shape of the clusters depend on both a type of a detected particle and its energy. This issue was studied using the Timepix pixels detectors with silicon sensor in [4, 6, 7]. Neutrons also could be accounted by registration of electrons and gammas resulting from the neutron induced activation of the sensor material (see section 2.3).

In figure 5 typical measured cluster size distributions of events recorded in the GPX7 detector for sensor thicknesses of 500 µm and 1000 µm are shown. More than 80% of the events have a size of no more than four pixels. Since the particle identification for clusters with small size is unreliable, the results presented below are obtained without particle identification procedure.

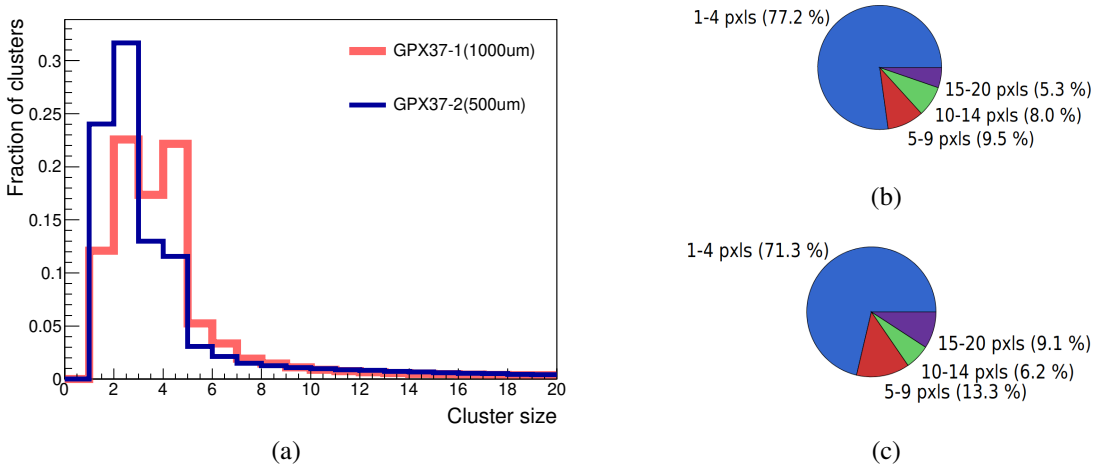

(a) (b) (c)

Figure 5. Measured cluster size distributions of events recorded in the GPX7 detector on 20.08.2018: (a) cluster size distribution in 500 µm and 1000 µm thick sensors; (b) fractions of cluster sizes in the 500 µm thick sensor; (c) fractions of cluster sizes in the 1000 µm thick sensor.

The data were recorded within 13 TeV proton-proton collisions during the LHC Run 2 (2017–2018). A typical count rate curve of the detectors (based on the average number of clusters per frame) in collisions-on and collisions-off periods is shown in figure 6.

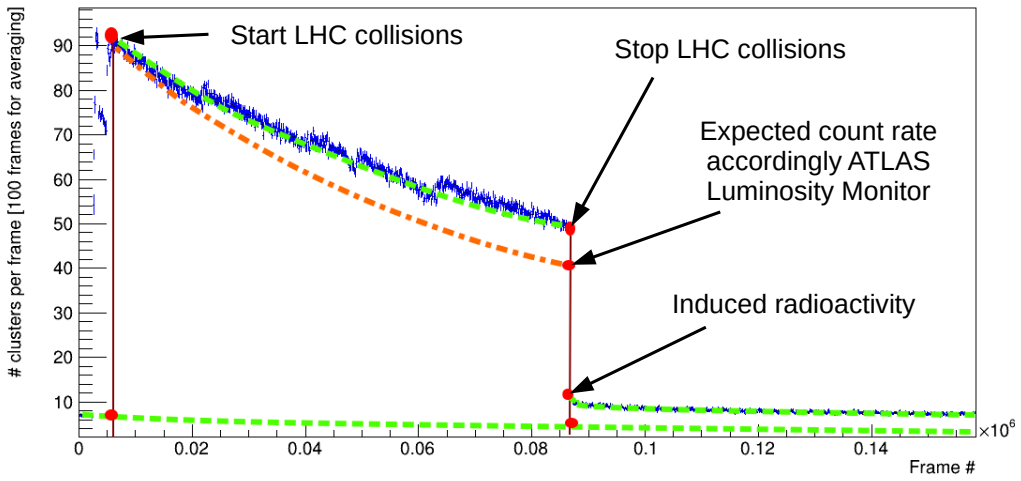

Figure 6. The cluster (event) rate of the GPX1 detector (blue) in collisions-on and collisions-off periods. The orange line is the expected cluster rate calculated in accordance with luminosity level at the ATLAS luminosity monitor. The green lines are fitted curves on the experimental data.

2021 JINST 16 P01031

One can see the high response from the start to the end of a luminosity cycle of LHC collisions. However, the decline of the GPX1 count rate is smaller than the decline of the LHC luminosity measured by the ATLAS luminosity monitor. The count rate of the detector is higher than this expected according to luminosity level (blue points and red line on figure 6 respectively). After the end of a luminosity cycle, the count rate in the GPX1 detector remains clearly non-zero and decreases with time. As will be argued below, this is explained by the effect of induced radioactivity in the materials in and around the detector.

2.2 Detector calibration

Before installation in the ATLAS cavern all GaAsPix detectors were tested using the standard energy calibration procedure [16, 17]. The global energy threshold was set as low as possible with a view to sensitivity for low energy γ's. A typical threshold value was 6.5 keV.

The detectors have been irradiated with huge intensities for months. That causes distractions inside the sensor material and electronics as well. Over time some pixels deteriorate and begin to noise. In order to avoid affecting of noisy pixels to the measurements the cleaning procedure is required. The idea was to look for pixels with count rates significantly higher than average using data collected in the periods without beams' collisions. In addition to the search the first five lines of pixels on the sensor edges were excluded from consideration.

2.3 Activation by neutron capture

Many materials in the ATLAS cavern are activated by particles released in the proton-proton collisions of the LHC [18]. It is very difficult to identify exactly which materials were activated, their precise locations, and their levels of activation as a function of time, because of a complexity of material elemental composition. On the other hand, the exact positions of the GaAsPix detectors in the cavern, their material composition, and many activation and decay modes of isotopes therein are known, notably the following ones:

$$
\begin{aligned}
&{}^{71}\mathrm{Ga} + \mathrm{n} \rightarrow {}^{72}\mathrm{Ga} \rightarrow \mathrm{e}^{-}\ (3{,}997\ \mathrm{MeV}) + {}^{72}\mathrm{Ge}\ (T_{1/2} = 14,11\ \mathrm{h}),\\
&{}^{75}\mathrm{As} + \mathrm{n} \rightarrow {}^{76}\mathrm{As} \rightarrow \mathrm{e}^{-}\ (2{,}962\ \mathrm{MeV}) + {}^{76}\mathrm{Se}\ (T_{1/2} = 26,26\ \mathrm{h}),\\
&{}^{69}\mathrm{Ga} + \mathrm{n} \rightarrow {}^{70}\mathrm{Ga} \rightarrow \mathrm{e}^{-}\ (1{,}65\ \mathrm{MeV}) + {}^{70}\mathrm{Ge}\ (T_{1/2} = 21,13\ \mathrm{m}).
\end{aligned}
$$

As shown in [4, 18] and [19], the radioactivity induced in surounding construction materials of the ATLAS experiment can be measured as a function of time by means of ATLAS-MPX and ATLAS-TPX detectors equipped with silicon sensors. However, in the case of GaAsPix detectors, one can expect that the measured signal will significantly increase by a signal corresponding to the radioactivity induced by the interactions of neutrons with the atomic nuclei of the elements contained in the GaAs Timepix detectors. Among them, the radioactivity induced by thermal neutrons as described by the equations above should play a dominant role.

3 Results and discussion

3.1 Normalised radiation levels in the period 2017–2018

In order to understand the radiation field in the cavern the responses of the detectors to radiation are normalised to the response of a specific detector, GPX7 (twin 1000/500 µm). The comparison

2021 JINST 16 P01031

is made separately for 500 µm and for 1000 µm thickness sensor layers for data collected during collisions. The cluster rate of each 1000 µm layer detector was normalised to the cluster rate of GPX7-1 (1000 µm), the cluster rate of 500 µm layer detectors — to GPX7-2's (500 µm). The data demonstrate reasonable stability with time permitting averaging over the entire running period 2017–2018 (see figure 7 and table 2).

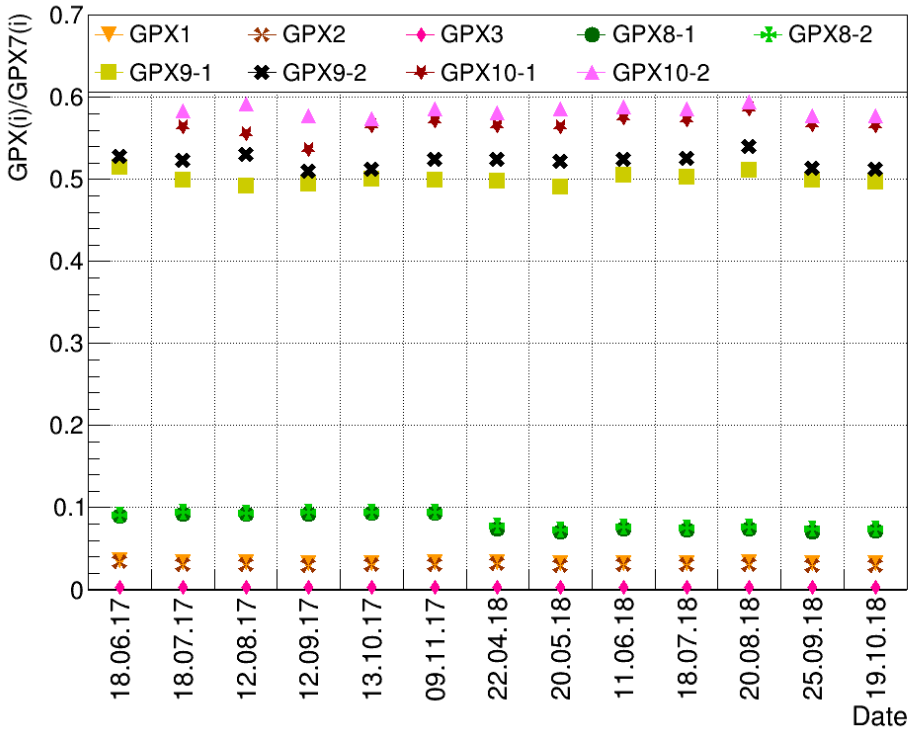

Figure 7. The cluster (event) counts of the GaAsPix detectors to radiation normalised to the cluster counts of the GPX7 detector. One point corresponds to the whole run in this date in the relevant detector.

Table 2. The responses of the GaAsPix detectors to radiation normalised to the responses of the GPX7 detector.

Detector#	$N_{\text{tot}}(GPXi)/N_{\text{tot}}(GPX7)$
GPX1	0.032 ± 0.001
GPX2	0.031 ± 0.002
GPX3	0.0029 ± 0.0002
GPX8-1	0.08 ± 0.01
GPX8-2	0.08 ± 0.01
GPX9-1	0.499 ± 0.007
GPX9-2	0.522 ± 0.008
GPX10-1	0.57 ± 0.01
GPX10-2	0.584 ± 0.006

3.2 Estimation of the charged and neutral radiation components

As shown above in figure 3, the twin GaAsPix detectors were assembled from two sensor layers with 500 µm and 1000 µm thickness, respectively. GaAsPix detectors with that thicknesses have nearly 100% detection efficiency for charged particles. However, for neutral particles (n, γ,. . .) the detection efficiency depends on the thickness of the sensors and on the particle energy (see figure 1).

Figure 8 shows the ratio of cluster count rates to radiation of thin (500 µm) to thick (1000 µm) GaAsPix sensor layers at the same location in the ATLAS cavern. The ratio is equal to unity for sensor layers with the same thickness, and is close to 1.7 for sensor layers with thickness different by a factor of two. The ratios are stable with time (the earliest data points from 27.05.2017 refer to the commissioning period and are ignored in the following analysis).

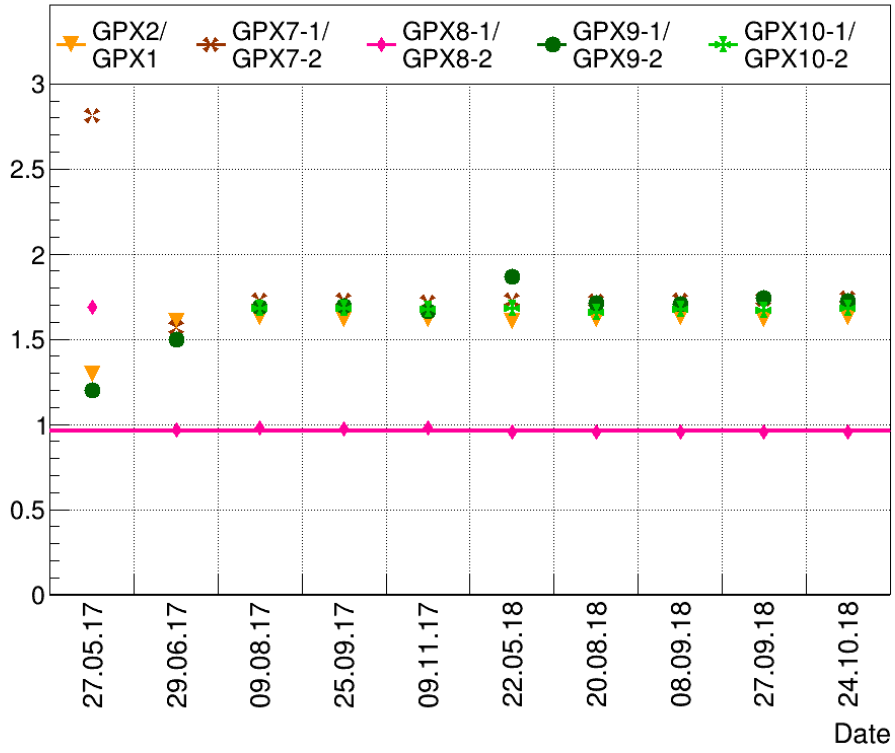

Figure 8. Ratio of cluster (event) counts of thick (1000 µm) to thin (500 µm) GaAsPix sensor layers at the same location in the ATLAS cavern.

An estimate of the ratio of charged and neutral radiation components can be made in assumption that the neutral radiation component is dominated by γ's with energy above 60 keV. For estimation the different thickness sensors response to charged and neutral particles is considered. Registration efficiency of charged particles in both sensors is 100%. Presuming the registration efficiency of neutral particles linearly depends on the sensor's thickness, i.e. the 500 µm sensors registers only a half of neutral particles in comparison with 1000 µm sensor. Assuming the total (full) efficiency of

2021 JINST 16 P01031

1000 µm sensor equals 1, one gets a simple system of equations:

$$N_{\text{neutral}}(1000) = 2\frac{1 - N_{\text{total}}(500)}{N_{\text{total}}(1000)}$$
$$N_{\text{charged}}(1000) = \frac{2N_{\text{total}}(500)}{N_{\text{total}}(1000)} - 1$$

The ratios of detector responses are the averages of the data shown in figure 8. The results of calculation of the equations above using the measured ratios are shown in table 3.

Table 3. Estimation of the charged and neutral radiation components.The ratio between the GPX8-1 and GPX8-2 sensor layers with equal thickness of 1000 µm is shown as demonstration of internal consistency.

Detector #	N_{tot} (1000 µm) / N_{tot} (500 µm)	$N_{charged}$	$N_{neutral}$
1 2	1.62 ± 0.04	0.24 ± 0.03	0.76 ± 0.03
7-1 7-2	1.7 ± 0.1	0.17 ± 0.09	0.83 ± 0.09
9-1 9-2	1.7 ± 0.1	0.18 ± 0.08	0.82 ± 0.08
10-1 10-2	1.676 ± 0.008	0.194 ± 0.006	0.806 ± 0.006
8-1 *8-2*	*0.96 ± 0.08*	-	-

3.3 Estimation of the neutron fluence by induced activity in the GaAsPix detectors

As already mentioned above, GaAsPix detectors have the potential of measuring neutron fluence by observing the decay products of radioactive isotopes that are activated by neutron capture in the detector material. For thermal neutrons with an energy below 1 eV, the cross-section of the (n, γ) reaction is of the order of 1–100 barn (see figure 1). A notable feature of the method is that the decay of the radioactive isotopes occurs within the sensor material and is detected with a much higher probability than the decay products of radioactive isotopes in the ATLAS structures surrounding the GaAsPix detector.

The data analysis proceeded in several steps. First of all, the ability must be shown to identify specific radioactive isotopes that are expected to be activated in GaAaPix detectors by neutrons: ^{72}Ga, ^{76}As, and ^{70}Ga. For this purpose, longer no beem periods of the LHC (at least 50 hours long), preferably preceded by data taking periods with high luminosity, must be selected. Three such periods were found: 30.06.2017–03.07.2017, 20.08.2018–23.08.2018, and 26.09.2018–29.09.2018. The time-dependence of the data from several GaAsPix detectors was fitted by the sum of four exponential decay distributions, three of them with the decay constants of the expected isotopes, and the fourth with an unknown decay constant (see figure 9):

$$f(t) = (P_0 + P_1 \exp(-\lambda_{\text{Ga72}} t) + P_2 \exp(-\lambda_{\text{As76}} t) + P_3 \exp(-\lambda_{\text{Ga70}} t) + P_4 \exp(-\lambda_4 t)$$

2021 JINST 16 P01031

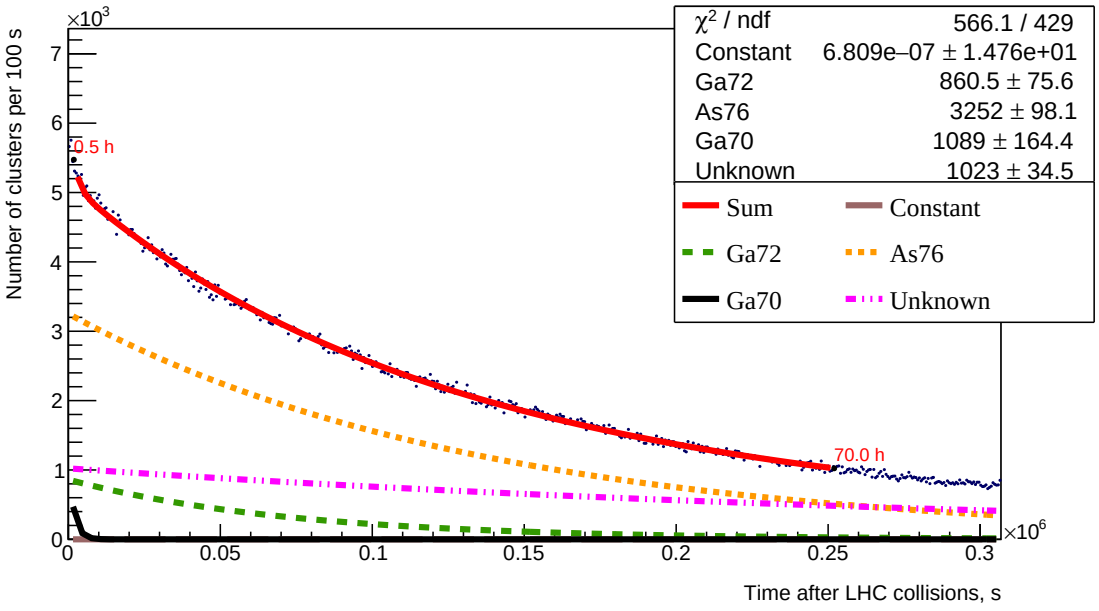

Figure 9. Fit of the time dependence of the response of GPX8-1 in the period 20.08.2018–23.08.2018 with a constant background and the sum of exponential decay curves.

The successful fit proves that it is possible to identify reliably expected well-known isotopes in the GaAsPix detector through their decay constants. The fourth component of the fit function was determined with a half-life of $T_{1/2} = 65$ h. To identify the origin of this component, tests were performed at the IBR-2 reactor in the Joint Institute for Nuclear Research in Dubna, Russia. The GPX8 detector was irradiated with thermal neutrons with energy $E_n < 0.05$ eV. The same long lived ($T_{1/2} = 65.5$ h) decay process was found. It is consistent with the decay of the ^{198}Au isotope produced in the ^{197}Au (n, γ) ^{198}Au capture reaction.

After breaking the GaAsPix detector into three parts (GaAs:Cr sensor layer, Timepix chip, and the support structure) and irradiating them again with thermal neutrons, it was ascertained that the source was a layer of gold in the Timepix chip probably coming from a layer used in preparing the pad of the chip for bump bonding. The reason why this tiny amount of gold gives rise to a signal that is comparable to the one from ~ 1 g of GaAs, is the rather huge cross-section of the ^{197}Au (n, γ) ^{198}Au reaction for thermal neutrons: for energies below 1 eV, it decreases slowly from 10^3 b to 10^2 b [14].

Table 4 presents the contributions of the four identified isotopes that are activated by the neutron radiation during LHC collision data taking. More than 90% of the overall detector response originates from these isotopes.

The separate identification of four different isotopes, each with a specific energy dependence of the (n, γ) cross-section, opens the prospect of an approximate reconstruction of the neutron energy spectrum.

2021 JINST 16 P01031

Table 4. Summary of neutron activation analyses.

Run	GPX	Const (p0)	^{72}Ga(p1)	^{76}As(p3)	^{70}Ga(p5)	Long (p7)	p1+p3+ p5+p7	Error
	1	5.8%	21.3%	0.0%	37.4%	35.5%	94.2%	2.9%
LHC	2	0.0%	38.2%	6.9%	43.3%	11.6%	100.0%	1.8%
30.06.17	7-1	0.0%	31.5%	19.0%	39.6%	9.9%	100.0%	1.1%
until	7-2	0.0%	30.4%	21.1%	39.6%	9.0%	100.0%	1.4%
03.07.17	8-1	0.0%	25.8%	33.6%	32.3%	8.4%	100.0%	0.4%
	8-2	0.0%	25.8%	31.2%	34.9%	8.1%	100.0%	1.8%
	9-1	0.0%	35.5%	20.2%	35.8%	8.5%	100.0%	1.6%
	9-2	0.0%	32.6%	24.7%	35.2%	7.5%	100.0%	2.1%
	1	0.0%	31.1%	1.1%	28.5%	39.3%	100.0%	3.1%
LHC	2	0.0%	28.3%	26.1%	28.6%	16.9%	100.0%	2.3%
20.08.18	7-1	0.0%	22.2%	33.6%	26.1%	18.1%	100.0%	2.8%
until	7-2	4.0%	10.7%	62.0%	21.9%	1.0%	96.0%	3.3%
23.08.18	8-1	0.0%	13.7%	52.5%	17.5%	16.2%	100.0%	3.4%
	8-2	0.0%	12.9%	52.4%	19.1%	15.6%	100.0%	3.4%
	9-2	0.0%	27.7%	27.5%	17.3%	27.4%	100.0%	5.6%
	1	8.3%	33.3%	0.0%	25.3%	33.1%	91.7%	2.9%
LHC	2	0.0%	33.5%	16.5%	31.9%	18.0%	100.0%	2.5%
26.09.18	5	0.0%	22.8%	29.9%	28.1%	19.2%	100.0%	3.2%
until	7-1	0.0%	24.5%	24.4%	33.7%	17.4%	100.0%	2.9%
29.09.18	7-2	0.0%	25.4%	26.7%	30.1%	17.8%	100.0%	4.0%
	8-1	0.0%	15.9%	43.9%	24.9%	15.3%	100.0%	3.6%
	8-2	0.0%	15.6%	42.7%	26.2%	15.4%	100.0%	3.6%
	9-2	7.3%	19.7%	55.1%	17.9%	0.0%	92.7%	74.5%
Thermal n	8-1	5.2%	0.0%	51.9%	10.5%	32.3%	94.8%	2.2%
(Reactor)	8-2	1.6%	0.0%	57.2%	6.2%	35.0%	98.5%	2.2%
Fast n	8-1	0.0%	18.9%	60.8%	19.8%	0.5%	100.0%	0.6%
(Reactor)	8-2	0.0%	19.4%	62.4%	18.0%	0.2%	100.0%	0.6%

4 Conclusions

- A network of ten GaAsPix detectors was produced, calibrated, and installed in the ATLAS cavern at the LHC, an environment of intense radiation during beam collisions. Data were accumulated in the years 2017–2018 and the operation of the detectors were stable and reliable.
- The network of GaAsPix detectors permits measuring and monitoring the radiation environment at different locations around the ATLAS detector. It can be seen from these data that the intensity distribution of the radiation environment around the ATLAS detector is quite stable during the entire measurement period (2017–2018 years).

2021 JINST 16 P01031

- The comparison of the responses from detectors with different sensor layer thicknesses (500 µm and 1000 µm) permits estimating the charged and neutral radiation components. This composition changes a little over the all time of measurements, which makes it possible to average these data. Within the error limits, the average ratio of the contributions of the charged and neutral components in the total radiation level is as 20% and 80%, respectively.

- The detector responses recorded during LHC shutdown periods arise from the decay of four specific isotopes that were activated in the GaAs material by neutrons during periods of beam collisions. The known decay constants and neutron capture cross-sections of these isotopes permit an estimate of the neutron fluence during beam collisions. Furthermore, activation of the detectors materials makes it possible to exclude the influence of neutron-induced activity in the materials surrounding GaAsPix detectors, the value of which is difficult to estimate at the locations of the detectors.

Acknowledgments

We thank Friedrich Dydak for useful and productive discussions. We also thank our colleagues from DLNP JINR (Dzhelepov Laboratory of Nuclear Problems at Joint Institute for Nuclear Research) Alexey Zhemchugov, Alexey Guskov and Dmitrii Dedovitch for productive discussions and significant help with choices of the data analysis procedure. We thank Sergey Borzakov, Yuriy Kopach and Egor Lychagin for help in measurements at neutrons beams at FLNP JINR (Frank Laboratory of Neutron Physics at Joint Institute for Nuclear Research). We thank Ian Dawson (University of Sheffield) and Mika Huhtinen (CERN) from the ATLAS Radiation Simulation work group for the considerable assistance and helpful advises. We also thank Sergey Malyukov and Marco Ciapetti from CERN for help in placing detectors and their cables in the ATLAS cavern. Special thanks to Dmitrii Grozdov for carring out the neutron activation analysis of the GaAs Timepix detector parts at FLNP JINR.

The work was supported from European Regional Development Fund-Project Engineering Applications of Microworld Physics (Contract Number CZ.02.1.01/0.0/0.0/16_019/0000766).

References

[1] L. Tlustos et al., *Characterisation of a GaAs(Cr) Medipix2 hybrid pixel detector*, *Nucl. Instrum. Meth. A* **633** (2011) S103.

[2] X. Llopart, R. Ballabriga, M. Campbell, L. Tlustos and W. Wong, *Timepix, a 65k programmable pixel readout chip for arrival time, energy and/or photon counting measurements*, *Nucl. Instrum. Meth. A* **581** (2007) 485 [*Erratum ibid.* **585** (2008) 106]

[3] D. Dedovich et al., *Proposal to Measure Radiation Field Characteristics, Luminosity and Induced Radioactivity in ATLAS with TIMEPIX detectors having GaAs:Cr sensors*, ATLAS internal note ATL-COM-GEN-2016-001 (2016).

[4] M. Campbell et al., *Analysis of the Radiation Field in ATLAS Using 2008 2011 Data from the ATLAS-MPX Network*, ATL-GEN-PUB-2013-001 (2013).

2021 JINST 16 P01031

[5] C. Leroy, S. Pospisil, M. Suk and Z. Vykydal, *Proposal to Measure Radiation Field Characteristics, Luminosity and Induced Radioactivity in ATLAS with TIMEPIX Devices*, ATLAS internal note ATL-COM-GEN-2014-005 (2014).

[6] B. Bergmann et al., *ATLAS-TPX: a two-layer pixel detector setup for neutron detection and radiation field characterization*, 2016 *JINST* **11** P10002.

[7] B. Bergmann et al., *Characterization of the Radiation Field in the ATLAS Experiment With Timepix Detectors*, *IEEE Trans. Nucl. Sci.* **66** (2019) 1861.

[8] B. Bergmann et al., *Relative luminosity measurement with Timepix3 in ATLAS*, 2020 *JINST* **15** C01039.

[9] P. Smolyanskiy et al., *Characterization of GaAs:Cr-based Timepix detector using synchrotron radiation and charged particles*, 2016 *JINST* **11** C12070.

[10] P. Smolyanskiy et al., *Study of a GaAs: Cr-based Timepix detector using synchrotron facility*, 2017 *JINST* **12** P11009.

[11] G. Chelkov et al., *Properties of GaAs:Cr-based Timepix detectors*, 2018 *JINST* **13** T02005.

[12] D. Kozhevnikov et al., *Performance and applications of GaAs:Cr-based Medipix detector in X-ray CT*, 2017 *JINST* **12** C01005.

[13] B. Bergmann et al., *Detector response and performance of a 500 µm thick GaAs attached to Timepix3 in relativistic particle beams*, 2020 *JINST* **15** C03013.

[14] NGATLAS, *Atlas of Neutron Capture Cross Sections*, https://www-nds.iaea.org/ngatlas2/.

[15] E. Ritsch, *Fast Calorimeter Punch-Through Simulation for the ATLAS Experiment*, MSc. thesis, University of Innsbruck, Innsbruck Austria (2011), https://cds.cern.ch/record/1388275/files/CERN-THESIS-2011-112.pdf.

[16] J. Jakubek, *Precise energy calibration of pixel detector working in time-over-threshold mode*, *Nucl. Instrum. Meth. A* **633** (2011) S262.

[17] A. Butler et al., *Measurement of the Energy Resolution and Calibration of Hybrid Pixel Detectors with GaAs:Cr Sensor and Timepix Readout Chip*, *Phys. Part. Nucl. Lett.* **12** (2015) 59.

[18] A. Sopczak et al., *Precision Measurements of Induced Radioactivity and Absolute Luminosity Determination with TPX Detectors in LHC Proton-Proton Collisions at 13 TeV*, *IEEE Trans. Nucl. Sci.* **65** (2018) 1371.

[19] M. Campbell et al., *Induced radioactivity in ATLAS cavern measured by MPX detector network*, 2019 *JINST* **14** P03010.

2021 JINST 16 P01031